





1992

# Thermo-Elastoviscoplastic Finite Element Plate Bending Analyses of Composites

Kwon, Y.W.

Monterey, California: Naval Postgraduate School.

Engineering Computations, Vol. 9, 595-607 (1992)

ENGINEERING COMPUTATIONS, VOL. 9, 595–607 (1992)

CONTRIBUTED Papers

# THERMO-ELASTOVISCOPLASTIC FINITE ELEMENT PLATE BENDING ANALYSES OF COMPOSITES

Y. W. KWON

*Department of Mechanical Engineering, Naval Postgraduate School, Monterey, CA 93943, USA*

## ABSTRACT

A formulation has been developed for thermo-elastoviscoplastic finite element analyses of continuous fibre-reinforced composite plates subject to bending loading using a generalized continuum mechanics approach. Such an approach is used to model the non-homogeneity in a composite, which is constituted by fibres embedded in a matrix material. The present formulation computes the respective stresses occurring in each constituent so that the respective yield criterion and flow rule of each constituent may be used if there is a material yielding in any constituent. Thermo-elastic deformation of fibre and thermo-elastoviscoplastic deformation of matrix are considered in the present study because the yield strength of fibre is substantially higher than that of matrix in many cases. Both constituents are assumed to be isotropic so that the von-Mises yield criterion may be used for viscoplastic yielding of matrix. As numerical examples, a parametric study is performed for thermo-elastoviscoplastic deformations of laminated composite plates subject to thermal bending loads.

KEY WORDS FE plate bending analyses Composite plates Bending loads

## INTRODUCTION

Most materials exhibit a more or less viscoplastic phenomenon. However, significance of such a phenomenon is quite different depending on materials and/or given environmental conditions. The same thing holds for composite materials. In particular, thermoplastic composites and metal–matrix composites exhibit quite a significant viscoplastic phenomenon at elevated temperatures. Temperature changes also induce thermal stresses in continuous fibre-reinforced composites, which consist of fibres embedded in matrix. The fibre and matrix, in general, have quite distinctive material properties. For example, fibre may have elastic deformation while matrix undergoes elastoviscoplastic deformation. This is a common phenomenon in fibre-reinforced composites because fibre has substantially quite higher yield strength than matrix. In such cases, elastoviscoplastic analysis of composite structures is not an easy task because of non-homogeneity of deformations. Furthermore thermal stresses in composities due to thermal loading make the analysis even more complicated.

0264–4401/92/060595–13$2.00

*Received March 1991*

Thermal stresses in composites can be investigated in terms of both micromechanical and macromechanical points of view. For instance, a unidirectional fibre-reinforced composite plate subject to a temperature change does not experience any stress at the macromechanical level if there is no constraint on the movement of the plate. However, at the micromechanical level there are thermal stresses in fibre and matrix, the resultant force of which is zero. It is due to a difference of thermal expansion coefficients of the two constituents. Therefore, thermal analyses of composites can be performed using either the micromechanical approach or the macromechanical approach. The macromechanical study is useful to determine deformed shapes of unsymmetrically laminated composite plates. An anticlastic warping of an unsymmetric cross-ply composite plate, with free edges and subject to a temperature change, was studied in Reference 1 using the classical plate bending theory. An anticlastic deformation of a composite was measured using an experimental technique, and the residual thermal stresses were measured by means of embedded strain gauges[2]. Hyer and his coworker[3–5] studied a bifurcation phenomenon of thermally deformed shapes of unsymmetric cross-ply composite plates. They found that an anticlastic shape of deformation in an unsymmetric cross-ply composite plate was stable under certain conditions and it was not stable under other conditions. For those cases, a deformed shape of cylindrical bending was the stable configuration. Thermoelastic deformations of symmetric and antisymmetric laminated plates with constrained edges were studied by Wu and Tauchert[6,7]. They computed transverse deflections of clamped and simply supported plates subject to a general three-dimensional temperature field.

Residual thermal stresses were also studied by many researchers[8–12]. Most of them calculated thermal stresses at the macromechanical level. These stresses are average stresses occurring in both fibre and matrix, and they were useful for the study of macromechanical failures of laminated composite plates. A macromechanical failure of a composite is related to micromechanical failures of fibre and matrix. For instance, a buckling failure of a composite structure is related to, more or less, to a micro-buckling or kinking of fibres[13–15]. Therefore, knowledge of stresses at the micromechanical level is also very important to study the strength of composites. However, the micromechanical study is usually limited to a very small local scale. As a result, both macromechanical and micromechanical approaches have their own merits as well as limitations.

Some analysis models were proposed in References 16–20, which filled a gap between the two approaches. Dvorak and his coworkers used the composite cylinder assemblage model[16,17] for composities under axisymmetric loads and the periodic hexagonal array model[18] for two-dimensional analyses of composites. Instantaneous stiffnesses of a composite plate were computed using the periodic hexagonal model at the micromechanics level. Since analytical computations were not easily obtainable, the finite element method was utilized to calculate the composite stiffnesses at material sampling points. It was an elaborate work. However, the formulation was computationally too expensive to be applied to a general composite structure. On the other hand, the analysis model used a generalized continuum mechanics[19,20]. The model assumed uniform stresses and strains in each constituent like the shear lag model[21]. Stresses and strains at the micromechanical level were related directly to those at the macromechanical. It was not as elaborate as the periodic hexagonal model, but it was computationally much more efficient.

All those papers considered two-dimensional problems. Because plates and shells are very common structural components, this paper presents a formulation for thermo-elastoviscoplastic analyses of composite plates under bending loads using a three-dimensional generalized continuum mechanics approach. A three-dimensional model is degenerated into an analysis model for a composite plate under a bending load, which is made of thermo-elastic fibres

embedded in a thermo-elastoviscoplastic matrix material. A thermo-elastoviscoplastic analysis is also an alternative way to solve a thermo-elastoplastic problem because the steady-state solution of a non-linear thermo-elastoviscoplastic problem is the thermo-elastoplastic solution of the same problem. The following section shows the mathematical formulation and the derivation of the corresponding finite element matrix equation. The resultant plate bending element has only translational degrees of freedom at nodes. This element was developed and tested in References 22–24. Numerical examples, which show a parametric study of thermo-elastoviscoplastic deformations of unidirectional composite plates and unsymmetrically laminated composite plates subject to thermal bending loads, and conclusions are followed.

## MATHEMATICAL DERIVATION OF ANALYSIS MODEL

A three-dimensional solid becomes a plate if the size in one dimension is much smaller than those in the other two dimensions. Consequently, a theory of plate bending can be derived from the theory of three-dimensional solid. In the classical plate bending theory, normal stress and strain components in the thickness direction as well as transverse shear stress and strain components are neglected even if some modified plate bending theories include some of those components. In the following derivation the normal stress and strain components are neglected, but the transverse shear deformation is included because it is quite important in laminated composite plates except for very thin plates.

The free body diagram of a three-dimensional solid element of a continuous fibre-reinforced composite is shown in *Figure 1*. Stress components on hidden sides of the element are not shown in the Figure. It is based on the following assumptions. The size of each fibre is infinitesimally small, fibres are embedded in a matrix material with uniform spacing, and the total volume of fibres constitutes a finite volume fraction of the composite. With body forces neglected, the equations of equilibrium are:

$$v^f \frac{\partial \sigma_1^f}{\partial x_1} + v^m \frac{\partial \sigma_1^m}{\partial x_1} + v^f \frac{\partial \tau_{12}^f}{\partial x_2} + v^m \frac{\partial \tau_{12}^m}{\partial x_2} + v^f \frac{\partial \tau_{13}^f}{\partial x_3} + v^m \frac{\partial \tau_{13}^m}{\partial x_3} = 0 \tag{1a}$$

$$v^f \frac{\partial \tau_{12}^f}{\partial x_1} + v^m \frac{\partial \tau_{12}^m}{\partial x_1} + \frac{\partial \sigma_2}{\partial x_2} + \frac{\partial \tau_{23}}{\partial x_3} = 0 \tag{1b}$$

$$v^f \frac{\partial \tau_{13}^f}{\partial x_1} + v^m \frac{\partial \tau_{13}^m}{\partial x_1} + \frac{\partial \tau_{23}}{\partial x_2} = 0 \tag{1c}$$

where subscripts 1 and 2 indicate longitudinal and transverse directions of fibres, subscript 3 indicates the thickness direction, superscripts $f$ and $m$ denote fibre and matrix respectively, and $v$ denotes a volume fraction. Stress component $\sigma_3$ is neglected in (1c). Similar equations can be also written for incremental stress components.

Total stress rates are related to total elastic strain rates by:

$$\{\dot{\sigma}^m\} = [E_e^m]\{\dot{\varepsilon}_e^m\} \tag{2a}$$

for fibre and

$$\{\dot{\sigma}^f\} = [E_e^f]\{\dot{\varepsilon}_e^f\} \tag{2b}$$

for matrix, where

$$\{\dot{\sigma}^m\} = \{\dot{\sigma}_1^m \quad \dot{\sigma}_2 \quad \dot{\tau}_{12}^m \quad \dot{\tau}_{23} \quad \dot{\tau}_{13}^m\}^T \tag{2c}$$

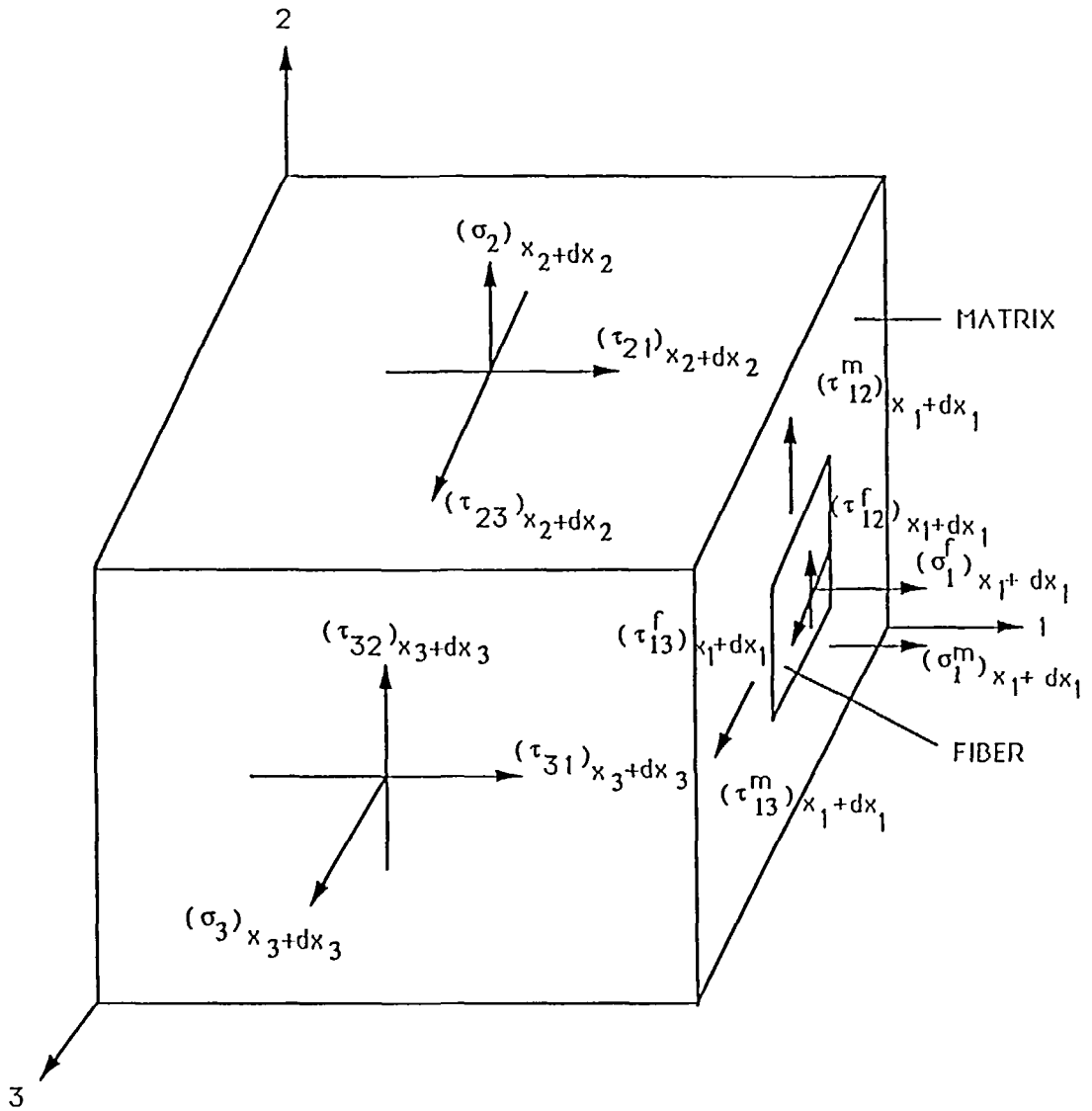


*Figure 1* Free body diagram of a fibre–matrix element

$$\{\dot{\sigma}^f\} = \{\dot{\sigma}^f_1 \quad \dot{\sigma}_2 \quad \dot{\tau}^f_{12} \quad \dot{\tau}_{23} \quad \dot{\tau}^f_{13}\}^T \tag{2d}$$

$$\{\dot{\varepsilon}^m_e\} = \{(\dot{\varepsilon}_e)_1 \quad (\dot{\varepsilon}^m_e)_2 \quad (\dot{\gamma}_e)_{12} \quad (\dot{\gamma}^m_e)_{23} \quad (\dot{\gamma}_e)_{13}\}^T \tag{2e}$$

$$\{\dot{\varepsilon}^f_e\} = \{(\dot{\varepsilon}_e)_1 \quad (\dot{\varepsilon}^f_e)_2 \quad (\dot{\gamma}_e)_{12} \quad (\dot{\gamma}^f_e)_{23} \quad (\dot{\gamma}_e)_{13}\}^T \tag{2f}$$

Superscript T indicates the transpose, and $[E^m_e]$ and $[E^f_e]$ are elastic material property matrices of matrix and fibre, respectively. The size of material property matrices is 5 × 5. Because the matrix has a thermo-elastoviscoplastic deformation, the total strain rate for the matrix is assumed to be decomposed into:

$$\{\dot{\varepsilon}^m\} = \{\dot{\varepsilon}^m_e\} + \{\dot{\varepsilon}^m_t\} + \{\dot{\varepsilon}^m_{vp}\} \tag{3}$$

where subscripts $e$, $t$, and $vp$ denote elastic, thermal, and viscoplastic strains. The generalized Duhamel–Neumann form of Hooke's law is used to relate thermo-elastic strain rates to stress rates. The viscoplastic strain rate of matrix may be written as:

$$\{\dot{\varepsilon}^m_{vp}\} = \mu\langle\Phi(Y)\rangle\frac{\partial Y}{\partial\{\sigma^m\}} \tag{4}$$

for the associated viscoplastic flow. Here $\mu$ is a fluidity parameter controlling the viscoplastic flow rate, and $Y$ is a scaler yield function of the matrix. The flow function $\langle\Phi(Y)\rangle$ is a positive monotonic increasing function for positive values of $Y$ only. For negative values of $Y$, $\langle\Phi(Y)\rangle$ is zero. A typical form:

$$\Phi(Y) = \left[\frac{Y - Y_o}{Y_o}\right]^b \tag{5}$$

is selected for the present study, where $Y_o$ is a uniaxial yield strength and $b$ is an arbitrarily prescribed constant. For fibre, the total strain rate is assumed to consist of elastic and thermal strain rates without viscoplastic deformation in the present formulation.

A stress increment in the matrix during $\Delta t_n$ is:

$$\{\Delta\sigma^m\}_n = [E^m_e](\{\Delta\varepsilon^m\}_n - \{\Delta\varepsilon^m_t\}_n - \{\Delta\varepsilon^m_{vp}\}_n) \tag{6}$$

in which $\{\Delta\varepsilon^m\}_n$ is a total strain increment, and a stress increment in the fibre is:

$$\{\Delta\sigma^f\}_n = [E^f_e](\{\Delta\varepsilon^f\}_n - \{\Delta\varepsilon^f_t\}_n) \tag{7}$$

A viscoplastic strain increment in the matrix is:

$$\{(\Delta\varepsilon^m_{vp})_n\} = [(1-\alpha)\{(\dot{\varepsilon}^m_{vp})_n\} + \alpha\{(\dot{\varepsilon}^m_{vp})\}_{n+1}](\Delta t_n) \tag{8}$$

during a time interval $\Delta t_n = t_{n+1} - t_n$, in which $\alpha$ is a parameter for time integration schemes. If $\alpha$ is zero, it results in fully explicit time integration scheme known as the Euler time integration scheme. A fully implicit time integration scheme is obtained for $\alpha = 1$. On the other hand, $\alpha = 0.5$ results in the Crank–Nicolson integration scheme. Numerical stability of the time integration schemes was discussed in detail by Owen and his coworkers[25,26]. The viscoplastic strain rate at time $t_{n+1}$ may be approximated as:

$$\{(\dot{\varepsilon}^m_{vp})_{n+1}\} = \{(\dot{\varepsilon}^m_{vp})_n\} + [H_n]\{(\Delta\sigma^m)_n\} \tag{9a}$$

where

$$[H_n] = \left[\frac{\partial\{(\dot{\varepsilon}^m_{vp})_n\}}{\partial\{\sigma\}^T}\right] \tag{9b}$$

Owen and Hinton[27] gave a detailed expression for matrix $[H_n]$ using the von Mises yield criterion for a three-dimensional solid. Matrix $[H_n]$ for plate bending can be obtained from that for a three-dimensional solid. Substitution of (9a) into (8) yields:

$$\{(\Delta\varepsilon^m_{vp})_n\} = \{(\dot{\varepsilon}^m_{vp})_n\}(\Delta t_n) + \alpha(\Delta t_n)[H_n]\{\Delta\sigma^m)_n\} \tag{10}$$

For the explicit time integration scheme, the second term on the right-hand side of (10) vanishes.

Substituting (10) into (6) gives an expression for a stress increment in terms of incremental strains as shown below:

$$\{\Delta\sigma^m\}_n = [E^m_{vp}](\{\Delta\varepsilon^m\}_n - \{\Delta\varepsilon^m_t\}_n - (\Delta t_n)\{(\dot{\varepsilon}^m_{vp})_n\}) \tag{11}$$

where

$$[E^m_{vp}] = ([\mathbf{I}] + \alpha(\Delta t_n)[E^m_e][H_n])^{-1}[E^m_e] \tag{12}$$

and [I] is the identity matrix. In order to relate strain increments $\Delta\varepsilon^f_2$ and $\Delta\varepsilon^m_2$ in the fibre and matrix respectively to the global strain increment $\Delta\varepsilon_2$, the following equation is used:

$$\Delta\varepsilon_2 = v^f(\Delta\varepsilon^f_2) + v^m(\Delta\varepsilon^m_2) \tag{13}$$

The transverse normal stress increment $\Delta\sigma_2$ is, from (7) and (11):

$$\begin{aligned}\Delta\sigma_2 &= (E^f_e)_{21}\Delta\varepsilon_1 + (E^f_e)_{22}\Delta\varepsilon^f_2 + (E^f_e)_{23}\Delta\gamma_{12} - (\Delta\sigma^f_t)_2 \\ &= (E^m_{vp})_{21}\Delta\varepsilon_1 + (E^m_{vp})_{22}\Delta\varepsilon^m_2 + (E^m_{vp})_{23}\Delta\gamma_{12} - (\Delta\sigma^m_t)_2 - (\Delta\sigma^m_{vp})_2\end{aligned} \tag{14}$$

where subscript $n$ is dropped for convenience, and stresses with subscripts $t$ and $vp$ are stress components in the transverse direction, which are associated with thermal and viscoplastic strains in (7) and (11). Solving (13) and (14) for $\Delta\varepsilon^f_2$ and $\Delta\varepsilon^m_2$ results in the following expressions for the local strains:

$$\begin{aligned}\Delta\varepsilon^f_2 = [&-v^m\{(E^f_e)_{21} - (E^m_{vp})_{21}\}\Delta\varepsilon_1 + (E^m_{vp})_{22}\Delta\varepsilon_2 - v^m\{(E^f_e)_{23} - (E^m_{vp})_{23}\}\Delta\gamma_{12} + \\ &v^m\{(\Delta\sigma^f_t)_2 - (\Delta\sigma^m_t)_2 - (\Delta\sigma^m_{vp})_2\}]/[v^m(E^f_e)_{22} + v^f(E^m_{vp})_{22}]\end{aligned} \tag{15a}$$

$$\begin{aligned}\Delta\varepsilon^m_2 = [&v^f\{(E^f_e)_{21} - (E^m_{vp})_{21}\}\Delta\varepsilon + (E^f_e)_{22}\Delta\varepsilon_2 + v^f\{(E^f_e)_{23} - (E^m_{vp})_{23}\}\Delta\gamma_{12} - \\ &v^f\{(\Delta\sigma^f_t)_2 - (\Delta\sigma^m_t)_2 - (\Delta\sigma^m_{vp})_2\}]/[v^m(E^f_e)_{22} + v^f(E^m_{vp})_{22}]\end{aligned} \tag{15b}$$

Similar expressions can be obtained for strains $\Delta\gamma^f_{12}$ and $\Delta\gamma^m_{12}$ like the following:

$$\Delta\gamma^f_{23} = [(E^m_{vp})_{44}\Delta\gamma_{23} - v^m(\Delta\tau^m_{vp})_{23}]/[v^m(E^f_e)_{44} + v^f(E^m_{vp})_{44}] \tag{16a}$$

$$\Delta\gamma^m_{23} = [(E^f_e)_{44}\Delta\gamma_{23} + v^f(\Delta\tau^m_{vp})_{23}]/[v^m(E^f_e)_{44} + v^f(E^m_{vp})_{44}] \tag{16b}$$

Substitution of (15a)–(16b) into (7) and (11) results in an expression relating micromechanical stress increments, $\{\Delta\sigma\} = \{\Delta\sigma^f_1, \Delta\sigma^m_1, \Delta\sigma_2, \Delta\tau^f_{12}, \Delta\tau^m_{12}, \Delta\tau_{23}, \Delta\tau^f_{13}, \Delta\tau^m_{13}\}^T$, to macromechanical strain increments, $\{\Delta\varepsilon\} = \{\Delta\varepsilon_1, \Delta\varepsilon_2, \Delta\gamma_{12}, \Delta\gamma_{23}, \Delta\gamma_{13}\}^T$.

## PLATE BENDING FINITE ELEMENT

In order to derive the corresponding finite element matrix equation, the Galerkin method is applied to (1a)–(1c) for incremental stresses $\{\Delta\sigma^f\}$ and $\{\Delta\sigma^m\}$ using displacements as test functions. These stress increments are expressed in terms of a global strain increment $\{\Delta\varepsilon\}$, which was obtained in the previous derivation. Finally, the global strain increment is replaced by a global displacement increment.

The plate bending element, which was developed and used in References 22–24, is used for the present study. The element has translational displacement components as nodal degrees of freedom but it has no rotational component as nodal degrees of freedom. Two inplane displacements, $u_1$ and $u_2$, vary linearly through the thickness, and the transverse displacement $u_3$ remains constant through the thickness. Therefore, interpolations of those displacements can be written as:

$$u_1 = \sum [N_i(\xi,\eta)H_1(\zeta)\bar{u}^i_1 + N_i(\xi,\eta)H_2(\zeta)\hat{u}^i_1] \tag{17a}$$

$$u_2 = \sum [N_i(\xi,\eta)H_1(\zeta)\bar{u}^i_2 + N_i(\xi,\eta)H_2(\zeta)\hat{u}^i_2] \tag{17b}$$

and

$$u_3 = \sum N_i(\xi, \eta) u_3^i \tag{17c}$$

where $^-$ and $^\wedge$ imply nodal displacements on top and bottom surfaces of a single unidirectional layer of a plate bending element, $N_i$ is a two-dimensional isoparametric shape function, and $H_i$ is the linear isoparametric shape function. The element stiffness matrix for a single layer of a plate bending element is:

$$[K] = \int_\Omega [B]^T [R]^T [D][B] \, d\Omega \tag{18a}$$

where

$$[R]^T = \begin{bmatrix} v^f & v^m & 0 & 0 & 0 & 0 & 0 & 0 \\ 0 & 0 & 1 & 0 & 0 & 0 & 0 & 0 \\ 0 & 0 & 0 & v^f & v^m & 0 & 0 & 0 \\ 0 & 0 & 0 & 0 & 0 & 1 & 0 & 0 \\ 0 & 0 & 0 & 0 & 0 & 0 & v^f & v^m \end{bmatrix} \tag{18b}$$

$[B]$ is the matrix relating strain increments to nodal displacement increments, and $[D]$ is the material property matrix relating $\{\Delta\sigma\}$ to $\{\Delta\varepsilon\}$ as explained in the previous section. The element stiffness matrix for a single layer is assembled over the total number of layers through the plate thickness. Reference 22 explains the assembly of element matrices and a condensation technique, to reduce the number of nodal degrees of freedom of plate elements, in detail.

## NUMERICAL EXAMPLES

The first set of examples is thermo-elastic deformations of unsymmetrically laminated plates with free edges subject to thermal loads. No mechanical loading is applied. Material properties used in the present study are given in *Table 1*, and the geometry of plates considered is shown in *Figure 2*. A deformed shape of a square, cross-ply composite plate with layers [90/0], subject to a temperature rise, is shown in *Figure 3*. The plate has the same size of thickness for each layer. The deformed surface is an anticlastic surface as well known in References 1–5. Deformations of rectangular plates with the same kind of layers are also illustrated in *Figure 4*. As aspect ratio $L_1/L_2$ becomes smaller, the curvature in one direction becomes smaller than

*Table 1* Material properties of fibre and matrix

| | |
|---|---|
| Elastic modulus of fibre | $60 \times 10^6$ lb/in$^2$ |
| Elastic modulus of matrix | $10 \times 10^6$ lb/in$^2$ |
| Poisson's ratio of fibre | 0.2 |
| Poisson's ratio of matrix | 0.33 |
| Yield strength of matrix | $12 \times 10^3$ lb/in |
| Thermal exp. coef. of fibre | $2.8 \times 10^{-6}$ °C$^{-1}$ |
| Thermal exp. coef. of matrix | $22.5 \times 10^{-6}$ °C$^{-1}$ |
| Fluidity parameter of matrix | $0.2 \times 10^{-3}$ h$^{-1}$ |

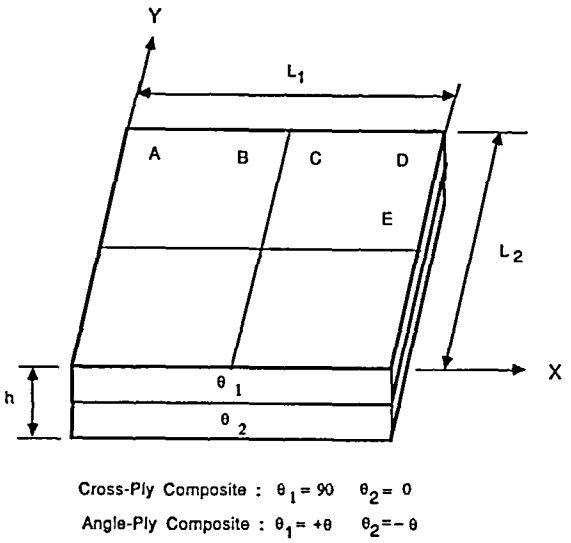


*Figure 2* Geometry of a laminated composite plate ($L_1/h = 100$) with a mesh of 2 × 2 eight-noded isoparametric elements

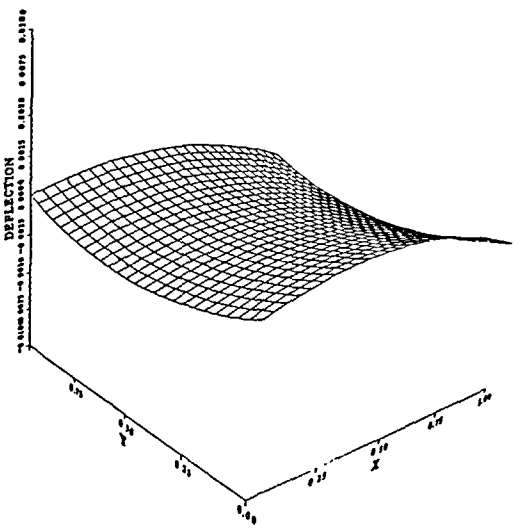


*Figure 3* Anticlastic deformation of a free, square composite plate with layers of [90/0]

that in the other direction. As a result, the deformed surface becomes closer to that of cylindrical bending as shown in *Figure 4*. Centres of the plates are assumed to have no displacement to prevent them from rigid body motions.

A unidirectional composite plate with free edges, subject to thermal loading, experiences thermal stresses at the micromechanical level. The micromechanical thermo-elastic stresses occurring in fibre and matrix can be computed from the following equations as given in Reference 1.

$$\sigma_L^f = E^f(\varepsilon_L - \varepsilon_t^f) \tag{19a}$$

$$\sigma_L^m = E^m(\varepsilon_L - \varepsilon_t^m) \tag{19b}$$

$$\varepsilon_L = [v^f E^f \varepsilon_t^f + v^m E^m \varepsilon_t^m]/[v^f E^f + v^m E^m] \tag{19c}$$

and subscript $L$ indicates the longitudinal direction. *Table 2* shows the micromechanical thermo-elastic stresses in the longitudinal direction occurring in fibre and matrix of a unidirectional composite plate subject to a unit temperature change and with various fibre volume fractions. Analytical solutions computed from (19a)–(19c) agree very well with the numerical solutions from the present model. For a temperature rise, fibre is in tension while matrix is in compression because the thermal expansion coefficient of matrix is larger than that of fibre in the present study. As shown in *Table 2*, the magnitude of matrix stress increases as the fibre volume fraction increases and the opposite is true for the fibre stress.

*Table 3* shows longitudinal, micromechanical stresses occurring in the unsymmetric, cross-ply composite plate considered above. Thermo-elastic stresses in the cross-ply composite are normalized with respect to those in a unidirectional composite with the same fibre volume fraction. The fibre stress is much larger near the middle surface (i.e. interface of layers) of the plate than near the top or bottom surface (i.e. free surface). However, the matrix stress is larger near the free surface. The variation of stress through the plate thickness is larger for fibre than

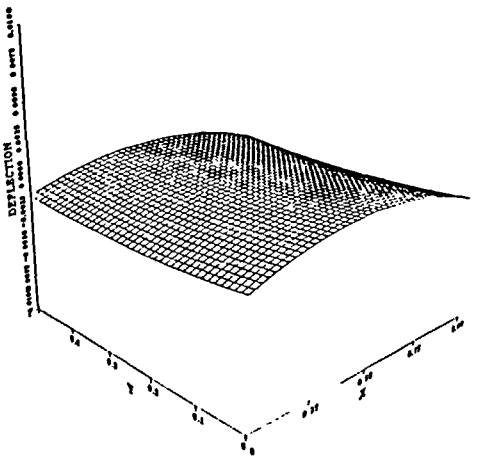


(a) $L_1 / L_2 = 2$

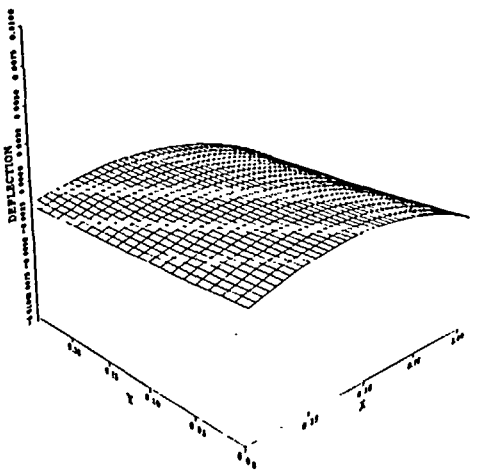


(b) $L_1 / L_2 = 4$

*Figure 4* Deformations of free, rectangular composite plates with layers of [90/0]

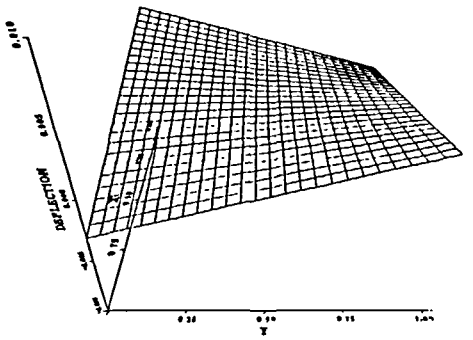


(a) θ=30

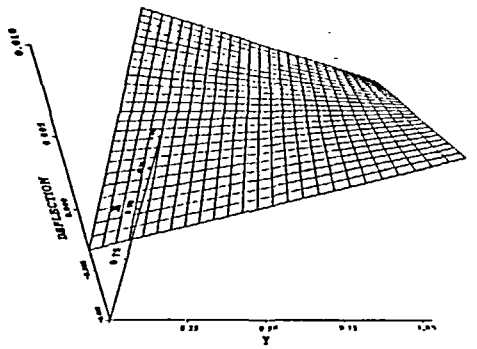


(b) θ=45

*Figure 5* Deformations of free, square composite plates with layers of $[\theta/-\theta]$

*Table 2* Longitudinal thermal stresses in unidirectional composite plate due to unit temperature rise

| Fibre vol. fraction | Fibre | Matrix |
|---|---|---|
| 0.4 | 236.4 | −157.6 |
| 0.45 | 200.0 | −163.7 |
| 0.5 | 168.9 | −168.9 |
| 0.55 | 141.8 | −173.4 |
| 0.6 | 118.2 | −177.3 |

*Table 3* Longitudinal thermal stresses in fibre and matrix of cross-ply composite plate

| | Fibre | | Matrix | |
|---|---|---|---|---|
| Fibre vol. fraction | Free surface | Interface | Free surface | Interface |
| 0.4 | 0.677 | 1.803 | 1.070 | 0.896 |
| 0.45 | 0.646 | 1.887 | 1.062 | 0.915 |
| 0.5 | 0.619 | 1.975 | 1.056 | 0.933 |
| 0.55 | 0.585 | 2.071 | 1.049 | 0.947 |
| 0.6 | 0.559 | 2.168 | 1.043 | 0.959 |

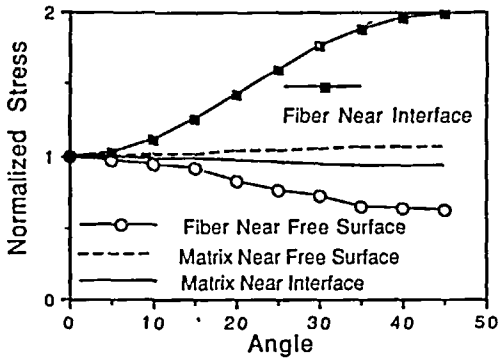


*Figure 6* Longitudinal stresses in angle-ply composite plate

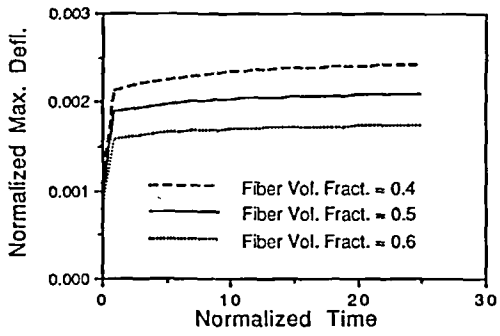


*Figure 8* Maximum deflection of cross-ply composite plat

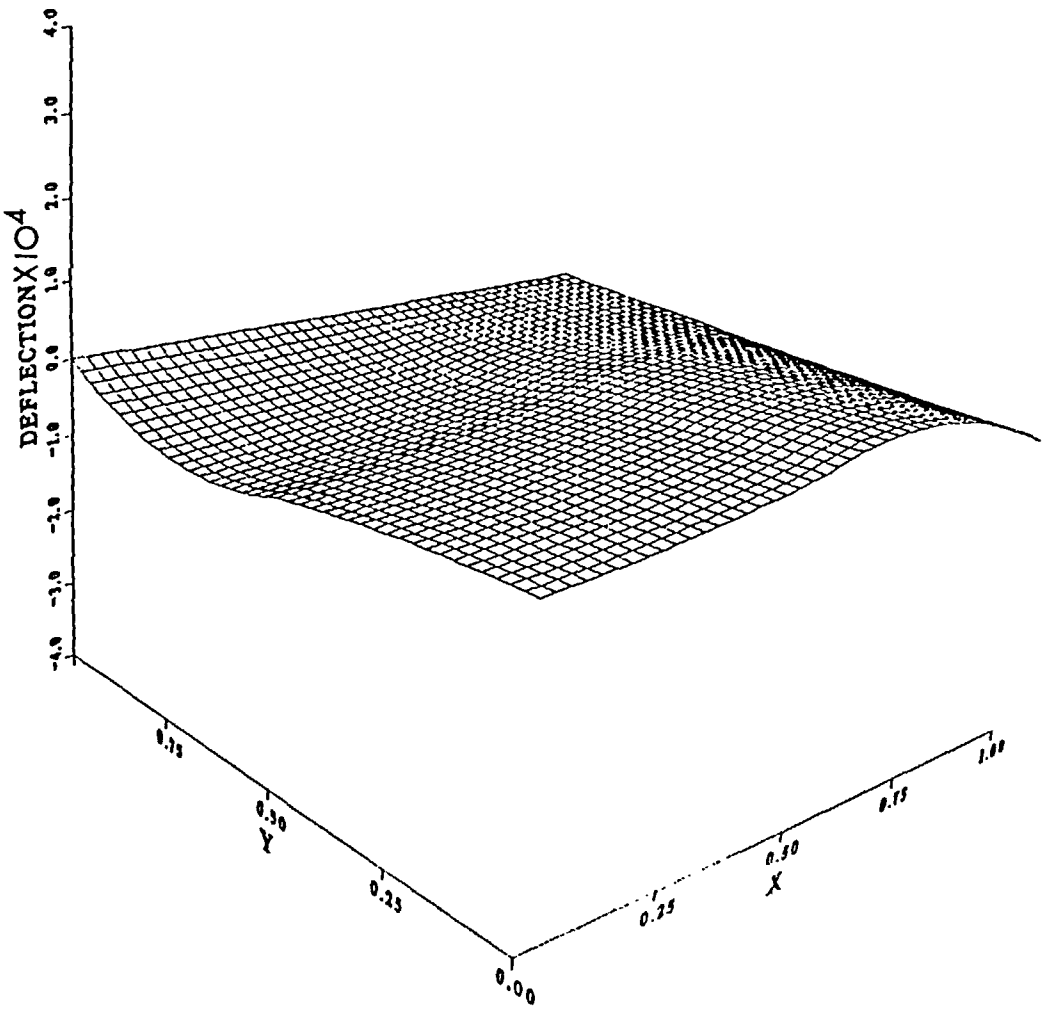


*Figure 7* Deformation of a simply supported, square composite plate with layers of [90/0]

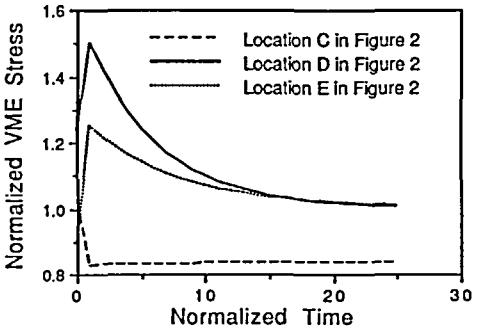


*Figure 9* von Mises equivalent stresses in matrix of a cross-ply composite

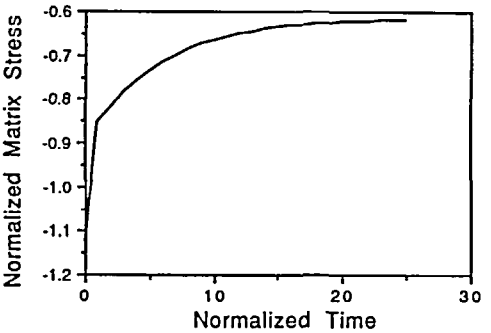


*Figure 10* Longitudinal matrix stress in cross-ply composite

for matrix. A large fibre volume fraction makes a larger change in the fibre stress as the plate changes from a unidirectional plate to a cross-ply plate. The opposite is true for the matrix stress. The change of matrix stress due to the change of layer orientation is not large compared to that of the fibre stress as shown in *Table 3.*

*Figure 5* illustrates deformed surfaces of two angle-ply composites. Centrepoints of the plates are again constrained to prevent them from rigid body motions. They are shown from the same view point. As shown in the Figure, the two plates have very similar deformed shapes even if there is a some difference in the magnitude of deformation. Variation of longitudinal fibre and matrix stresses is given in *Figure 6* with a change of layer angle in angle-ply composites with layers of $[\theta/-\theta]$. Those stresses are normalized with respect to the stresses in a unidirectional composite. The fibre stress increases near the interface of the two layers and it decreases near the free surface as the angle, $\theta$, increases from 0° to 45°. On the other hand, the matrix stress decreases near the interface and it increases near the free surface as the angle increases. There is a large variation in fibre stresses than in matrix stresses. The fibre stress near the interface has the largest variation.

The next set of examples is thermo-elastoviscoplastic deformation of a cross-ply composite plate with simply supported edges. A square plate is considered. The deformed shape of the elastic plate due to a uniform temperature rise is shown in *Figure 7.* A quarter of the plate is shown because of symmetry. The characteristic of the deformed shape is the same as that given in Reference 7 with zero deflection along the diagonal. *Figure 8* is the progress of the maximum transverse deflection of the plate, subject to a temperature rise of 50°, as time elapses. Cases with three different fibre volume fractions are compared in the Figure. The maximum deflection is normalized such that the normalized deflection is $(u_3)_{max}D/M_pL^2$, in which $D$ is the plate rigidity in terms of the matrix material, $M_p$ is the plastic bending moment, and $L$ is a side length of the square plate. The normalized time is 5000 $\mu t$, in which $t$ is time. As expected, the smaller fibre volume fraction yields a larger deflection. The deflections approach the steady-state solutions. The characteristic deformed shape throughout the thermo-elastoviscoplastic deformation remains the same as that of the thermo-elastic deformation as shown in *Figure 7.*

Von Mises equivalent stresses occurring in matrix with a fibre volume fraction of 0.5 are given in *Figure 9.* The stresses are normalized with respect to the matrix yield strength, and they are computed very near the corner of the boundary. *Figure 10* shows the normalized, longitudinal matrix stress at location *D* of *Figure 2.* The yielding zone in the matrix material at the steady-state is located near and along the boundary edges, which are parallel to the fibre direction in each

*Table 4* Normalized longitudinal fibre stress in 90 degree ply of cross-ply composite with simply supported edges

| Fibre volume fraction | | Location in *Figure 2* | | | |
|---|---|---|---|---|---|
| | | A | B | C | D |
| 0.4 | Free surf. | 3.226 | 3.412 | 3.254 | 0.950 |
| | Interface | 4.969 | 5.087 | 4.547 | 1.261 |
| 0.5 | Free surf. | 2.564 | 2.689 | 2.550 | 0.640 |
| | Interface | 4.031 | 4.128 | 3.660 | 0.905 |
| 0.6 | Free surf. | 2.032 | 2.140 | 2.022 | 0.408 |
| | Interface | 3.251 | 3.333 | 2.942 | 0.627 |

layer. The longitudinal fibre stresses in the 90 degree-ply are tabulated in *Table 4* for different fibre volume fractions. Those stresses are also normalized with respect to the matrix yield strength. It shows that the fibre stress is relatively small near the free edges, which are parallel to $y$-axis.

## CONCLUSIONS

A mathematical formulation has been developed for thermo-elastoviscoplastic analyses of fibre-reinforced composite plates under bending loads, along with its finite element formulation. The formulation considered thermo-elastically deformed fibres embedded in a thermo-elastoviscoplastically deformed matrix material. The formulation was derived from the equations for a three-dimensional solid. A three-dimensional solid element type of plate bending element was also used for the finite element formulation. Advantage of the present formulation is that the two distinct material behaviours of fibre and matrix can be easily incorporated in the analysis model. In addition, stresses occurring in fibre and matrix can be computed separately and directly so that each constituent can use its own yield function and flow rule if the constituent yields. The proposed analysis model was demonstrated to be quite useful for thermo-elastoviscoplastic analyses of composite plates under bending loads through a study of example problems.

## ACKNOWLEDGEMENT

This paper was prepared in conjunction with research funded by the Naval Postgraduate School.

## REFERENCES

1 Tsai, S. W. and Hahn, H. T. *Introduction to Composite Materials*, Technomic, Westport, CT (1980)
2 Zewi, I. G., Daniel, I. M. and Gotro, J. T. Residual stresses and warpage in woven-glass/epoxy laminates, *Exp. Mech.*, pp. 4–50 (March 1987)
3 Hyer, M. W. Calculations of the room-temperature shapes of unsymmetric laminates, *J. Compos. Mat.*, **15**, 296–310 (1981)
4 Hyer, M. W. The room-temperature shapes of four-layer unsymmetric cross-ply laminates, *J. Compos. Mat.*, **16**, 318–340 (1982)
5 Hamamoto, A. and Hyer, M. W. Nonlinear temperature-curvature relationships for unsymmetric graphite-epoxy laminates, *Int. J. Solids Struct.*, **23**, 919–935 (1987)
6 Wu, C. H. and Tauchert, T. R. Thermoelastic analysis of laminated plates. 1: Symmetric specially orthrotropic laminates, *J. Thermal Stresses*, **3**, 247–259 (1980)

7 Wu, C. H. and Tauchert, T. R. Thermoelastic analysis of laminated plates. 1: Antysymmetric cross-ply and angle-ply laminates, *J. Thermal Stresses*, **3**, 365–378 (1980)
8 Hahn, H. T. and Pagano, N. J. Curing stresses in composite laminates, *J. Compos. Mat.*, **9**, 91–106 (1975)
9 Pagano, N. J. and Hahn, H. T. Evaluation of composite curing stresses, *ASTM STP 617*, pp. 317–329 (1977)
10 Jeronimidis, G. and Parkyn, A. T. Residual stresses in carbon fiber-thermoplastic matrix laminates, *J. Compos. Mat.*, **22**, 401–415 (1988)
11 Kural, M. H. and Min, B. K. The effects of matrix plasticity on the thermal deformation of continuous fiber graphite/metal composites, *J. Compos. Mat.*, **18**, 519–535 (1984)
12 Voyiadjis, G. Z. and Hartley, C. S. Residual-stress determination of concentric layers of cylindrically orthotropic materials, *Exp. Mech.*, pp. 290–297 (September 1987)
13 Rosen, B. W. Mechanics of composite strengthening, *Fiber Composite Materials*, American Society for Metals, pp. 37–75 (1965)
14 Evans, A. G. and Adler, W. F. Kinking as a mode of structural degradation in carbon fiber composites, *Acta Metallurg.*, **26**, 725–738 (1978)
15 Budiansky, B. Micromechanics, *Comp. Struct.*, **17**, 3–12 (1983)
16 Dvorak, G. J. and Rao, M. S. M. Axisymmetric plasticity theory of fibrous composites, *Int. J. Eng. Sci.*, **14**, 361–373 (1976)
17 Dvorak, G. J. and Rao, M. S. M. Thermal stresses in heat-treated fibrous composites, *J. Appl. Mech.*, **43**, 361–373 (1976)
18 Wu, J. F., Shephard, M. S., Dvorak, G. J. and Bahei-El-Din, Y. A. A material model for the finite element analysis of metal matrix composites, *Compos. Sci. Technol.*, **35**, 347–366 (1989)
19 Kwon, Y. W. and Byun, K. Y. Development of a new finite element formulation for the elasto-plastic analysis of fiber-reinforced composites, *Comp. Struct.*, **35**, 563–570 (1990)
20 Kwon, Y. W. Elasto-viscoplastic analysis of fiber-reinforced composites, *Eng. Comput.*, in press
21 Hedgepeth, J. M. Stress concentrations in filamentary structures, *NASA TND-882*, National Aeronautics and Space Administration, Langley (1961)
22 Owen, D. R. J. and Li, Z. H. A refined analysis of laminated plates by finite element displacement methods—I. Fundamentals and static analysis, *Comp. Struct.*, **26**, 907–914 (1987)
23 Owen, D. R. J. and Li, Z. H. A refined analysis of laminated plates by finite element displacement methods—II. Vibration and stability, *Comp. Struct.*, **26**, 915–923 (1987)
24 Kwon, Y. W. Finite element analysis of crack closure in plate bending, *Comp. Struct.*, **32**, 1439–1445 (1989)
24 Owen, D. R. J. and Liu, G. Q. Elasto-viscoplastic analysis of anisotropic laminated plates and shells, *Eng. Comput.*, **2**, 90–95 (1985)
25 Owen, D. R. J. and Damjanic, F. Viscoplastic analysis of solids: stability considerations, in *Recent Advances in Nonlinear Computational Mechanics*, (Ed. E. Hinton, D. R. J. Owen and C. Taylor), Pineridge Press, Swansea (1982)
26 Owen, D. R. J. and Hinton, E. *Finite Elements in Plasticity: Theory and Practice*, Pineridge Press, Swansea (1980)